

Article

An Integrated Remote Sensing and GIS-Based Technique for Mapping Groundwater Recharge Zones: A Case Study of SW Riyadh, Central Saudi Arabia

Eman Mohamed M. EL-Bana ¹, Haya M. Alogayell ¹, Mariam Hassan Sheta ² and Mohamed Abdelfattah ^{3,4,*} 

¹ Department of Geography and Environmental Sustainability, College of Humanities and Social Sciences, Princess Nourah bint Abdulrahman University, P.O. Box 84428, Riyadh 11671, Saudi Arabia

² Environmental Sciences Department, Faculty of Science, Port Said University, Port Said 42522, Egypt; mariam_sheta@sci.psu.edu.eg

³ Geology Department, Faculty of Science, Port Said University, Port Said 42522, Egypt

⁴ EDYTEM, University Savoie Mont-Blanc, 73370 Le Bourget du Lac, France

* Correspondence: mohamed_abdelfattah@sci.psu.edu.eg or mohamed.abdelfattah@univ-smb.fr

Abstract: It might be difficult to find possible groundwater reservoir zones, especially in arid or hilly regions. In the twenty-first century, remotely sensed satellite imagery may present a new opportunity to locate surface and subsurface water resources more quickly and affordably. In order to identify groundwater potential zones, the current study was conducted in Central Saudi Arabia, southwest of Riyadh. The present analysis employed a multi-criteria approach that relies on remote sensing and geographic information systems. The variables employed in this technique include geology, rainfall, elevation, slope, aspect, hillshade, drainage density, lineaments density, and Land Use/Land Cover (LULC). The Analytical Hierarchical Process (AHP) was used for assigning weights to the parameters, and the corresponding significance of each parameter's several classes for groundwater potentiality. Different groundwater potential zones were identified by the study: very high (16.8%), high (30%), medium (26.7%), low (18.6%), and very low (7.9%). Only two of the observation wells were located in the "medium" potential zone, but the other ten wells were observed in the "very high and high" potential zones, according to the validation survey. Consequently, the results may demonstrate that the current approach, which combines improved conceptualization with AHP to define and map groundwater potential zones, has a greater chance of producing accurate results and can be used to reduce the threat of drought in broader arid regions.

Keywords: remote sensing; GIS; multicriteria; groundwater potential zones; SW Riyadh; Saudi Arabia



Citation: EL-Bana, E.M.M.; Alogayell, H.M.; Sheta, M.H.; Abdelfattah, M. An Integrated Remote Sensing and GIS-Based Technique for Mapping Groundwater Recharge Zones: A Case Study of SW Riyadh, Central Saudi Arabia. *Hydrology* **2024**, *11*, 38. <https://doi.org/10.3390/hydrology11030038>

Academic Editors: Augustina Clara Alexander and Pantelis Sidiropoulos

Received: 24 January 2024

Revised: 27 February 2024

Accepted: 29 February 2024

Published: 3 March 2024



Copyright: © 2024 by the authors. Licensee MDPI, Basel, Switzerland. This article is an open access article distributed under the terms and conditions of the Creative Commons Attribution (CC BY) license (<https://creativecommons.org/licenses/by/4.0/>).

1. Introduction

Water access is essential for socioeconomic growth. Freshwater availability has historically served as a crucial indication of human prosperity and is important for achieving sustainable development objectives. However, in recent years, there has been a widespread worsening of water availability due to rapid population growth, high water requirements for construction, industrialization, and irrigation. Furthermore, freshwater availability has declined due to global climate change in many areas, including developing nations, especially in arid and semi-arid regions [1,2].

The primary supply of freshwater for a variety of applications is groundwater [3,4]. Prior research found that 26% of the world's sustainable freshwater sources come from groundwater [5]. Approximately 50% of the world's water requirements for residential use come from groundwater, which serves as the main source of water for industry, households, and agriculture, according to other studies [6,7]. In the majority of African communities, particularly those in dry and semi-arid regions, groundwater is one of the most valuable natural resources. Roughly 20% of the water utilized for agriculture, 40% for industry, and

50% for potable consumption comes from groundwater supplies [8]. Consequently, it is necessary to investigate these priceless resources for those who frequently have no other possibilities. Thus, it is critical to have a thorough grasp of groundwater systems over location and time. Groundwater reserves are subject to significant fluctuations in availability within short timeframes. This also holds true when research shows that groundwater resources are still not sufficiently investigated to satisfy the community's high demands [9]. Groundwater fills the pore spaces, cavities, and joints in the soil that are found inside rocks and geologic strata. The occurrence and infiltration of groundwater in rocks is determined by the hydraulic conductivity of the materials due to their lithologic properties such as porosity, permeability, and fluid transport via geologic structures [10–12]. Consequently, the two standard approaches for locating groundwater are drilling and geoelectric observation, both of which are quite costly and time-consuming.

As numerous studies have demonstrated, aquifer recharge zones are currently identified globally using the integration of remote sensing (RS) and geographic information system (GIS) techniques [13–16]. By considering similarities with the research region, these studies successfully identify the most advantageous locations for aquifer recharge [17–28]. A variety of characteristics have been used to define global potential zones, including rainfall, topography, lithology, geomorphology, slope, drainage pattern, and lineaments. Multi-criteria evaluation (MCE) is a widely utilized technique that is frequently used to assess various criteria together, and the results of this methodology offer persuasive proof of the aquifer's state [29–34].

GIS and remote sensing (RS) have the potential to be employed for groundwater investigation, as well as for regional predictions [35,36]. Big geographical data may be aggregated and analyzed to forecast and find new water sources by using GIS-based technology and/or data-driven methodologies [37,38]. Several research projects have demonstrated the practicality of combining GIS and RS to locate possible groundwater resource locations [35,39–41]. Several researchers have adopted and used a variety of methods for identifying groundwater potential zones (GWPZ), including the logistic regression model [42], random forest model [43], and frequency ratio [28,44]. The GIS and RS-based analytical hierarchy process (AHP) is considered a simple, effective, reliable, and cost-effective approach in this case [45–47]. Saaty (1977) gave the first explanation of AHP [48]. The intended outcomes are obtained by the AHP technique, which reduces complex results to a set of paired data [49]. It is commonly acknowledged that AHP is a very powerful method for assessing output reliability, reducing bias, and applying it in an innovative setting [50]. In order to evaluate aquifer potential and identify recharge zones, it is imperative that prior parameters, including rainfall, geology, geomorphology, slope, lineament density, and drainage density, be integrated into the weight overlay model. This comprehensive method uses the AHP to compute weightage, allowing for a more accurate evaluation of the aquifer's prospects as well as the identification of areas with notable recharging capability. Numerous investigations have been conducted worldwide to determine the groundwater potential zones using GIS and RS for the evaluation of groundwater resources in the Maknassy basin, Tunisia [51], Ghana [52], Burdur, Turkey [53], Egypt [54,55], Saudi Arabia [56], Kurdistan region, Iran [57], West Bengal, India [58], Eritrea [59], Uganda [60], Kenya [61], Huay Sai area, Thailand [62], and China [63].

The arid environment of the Kingdom of Saudi Arabia (KSA) makes renewable water resources scarce [64]. These limited water supplies and growing unpredictability brought on by climate change present significant problems for water management in the KSA. Another negative impact of using underground water from aquifers is the depletion of resources which have taken decades to recover again because the current annual rainfall has no direct effect [65,66]. The nation receives an estimated 158.47 billion m³ of rainwater yearly [67]. According to the previous studies, the largest single alluvial reservoir in the KSA has an overall capacity of 84 billion m³ [68–70]. Over the past two decades, about 254.5 billion m³ of groundwater has been utilized from Saudi Arabia's aquifers to satisfy the needs of the country's expanding agricultural industry [67]. However, over the past

20 years, only 41.04 billion m³ of water has been recharged into the deep aquifers [67]. The KSA's main supply of drinkable and agricultural water comes from groundwater [71,72]. Of the country's water requirement, 80% is met by the 17 billion m³/year of groundwater extracted in the KSA over the previous thirty years [71–73]. The KSA developed a plan to reduce the amount of water needed for agriculture by using modern irrigation techniques in order to adhere to the water preservation strategy [74]. The amount of water utilized for agriculture has decreased by 2.5% on average each year as a result of this strategy. It is essential to assess groundwater potential zones for agricultural expansion due to the limitations on the supply of water and the potential for growing the cultivated area.

Therefore, this study used a wide range of modern RS and GIS tools for broad investigation with the goal of identifying the groundwater promising zones and the most suitable spots for groundwater recharge. In the current study, the most effective groundwater recharge potentiality zones were predicted by processing and combining data from numerous satellite images, involving Shuttle Radar Topography Mission (STRM) and Landsat imagery. Utilizing GIS spatial analysis, several layers including topography, geology, soil, slope drainage density, LULC, and lineament maps were combined. The optimal groundwater recharge spots are successfully determined by this method. Water management in the research area is greatly aided by the findings from potential zone maps' classification into five zones, ranging from extremely high to very low groundwater recharge potential zones, using the GIS reclassification tool. The accuracy of the resultant map, which displays several neglected groundwater-capable places, is verified using drill wells. The groundwater potential zone (GWPZ) map can be used by developers and other stakeholders to direct future development. It is a crucial input for the use of sustainable agriculture in the interim. This study aims to map the distribution of shallow aquifers that facilitate industrial development, agriculture, and human settlement. This is accomplished by identifying locations in the Saudi Arabian province of SW Riyadh where aquifer recharge takes place, thoroughly evaluating the parameters that influence aquifers, and, in the end, creating a GWPZ map using MCE methodologies.

2. The Study Area

The study area was located in the geographical region of Al-Riyadh in central Saudi Arabia, roughly 150 km southwest of the country's capital, Riyadh (Figure 1a). Figure 1b shows the location of the wells. It has a surface area of 2340 km², and its elevation varies in altitude, starting at 645 m above sea level downstream of the region (the eastern part) to about 1277 m at the highest point of the watershed (the western section) (Figure 1c).

Saudi Arabia's terrain is mostly made up of harsh desert regions with hot temperatures. The research region exhibits a very warm climate, especially from May to September when monthly mean temperatures can reach above 30 °C (Figure 2a). In the KSA, the annual average precipitation ranges from 50 to 100 mm [75]. Riyadh and the Red Sea coast have the highest rates of rainfall in January, March, and April (Figure 2b). At Riyadh, the daily evaporation maximum in the summer may exceed 18.5 mm/day, with an average yearly evaporation of 2900 mm [75].

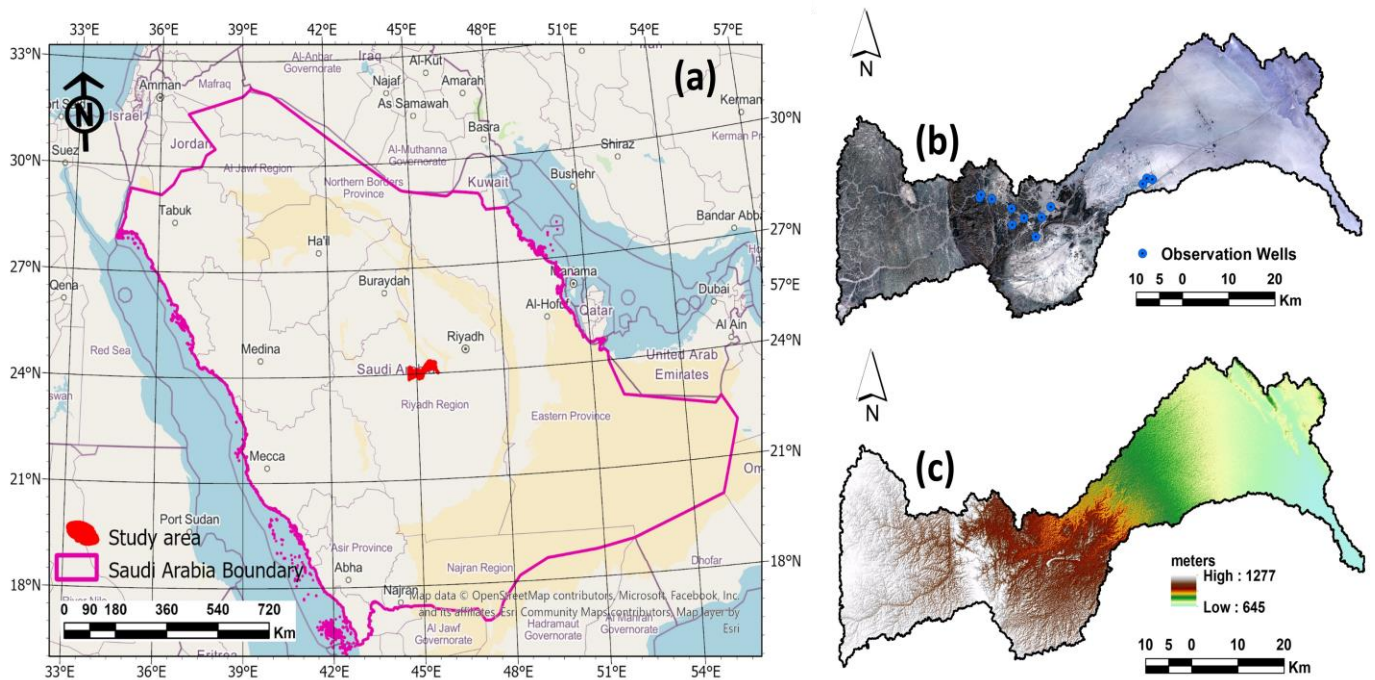


Figure 1. (a) Map showing the location of the study area in Saudi Arabia's boundary (b) Recent landsat-8 image showing the locations of wells (c) Digital Elevation Model of the study area.

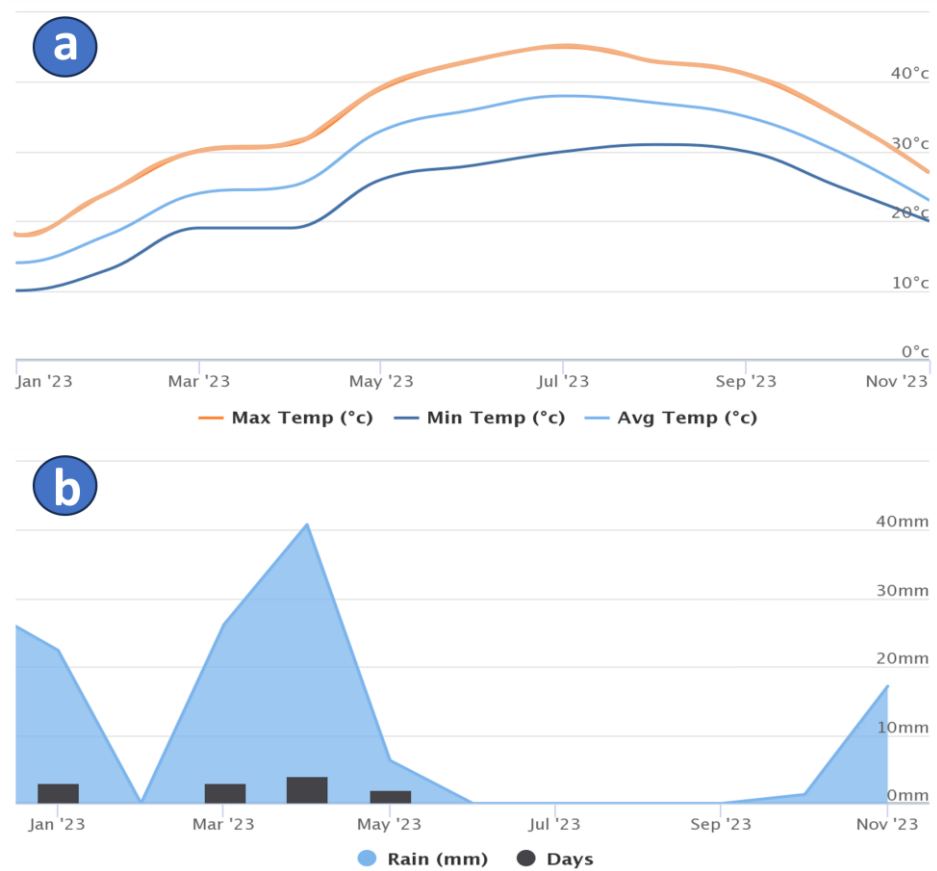


Figure 2. (a) The monthly temperature and (b) The monthly rainfall of the study area during 2023 [76].

Geological and Hydrogeological Setting

Tectonically, the Arabian Plate is where the KSA is located. Rocks that have undergone Late Precambrian metamorphism, both volcanic and volcano-sedimentary, comprise its composition [75]. The regional split of the plate is composed of two geological regimes: the Arabian Platform and the Arabian Shield. The Arabian Shield basements' tilt is the reason for this strata's eastern dip towards the Arabian Gulf [75]. The following characteristics make up the subsurface geology of the study area (Figure 3) [75]:

1. Rocks that are colluvial, alluvial, aeolian, and superficial. In the western section, quaternary sediments comprise an unconfined aquifer, while in the eastern region, they constitute a confined aquifer.
2. The Ash Shiqqah of the Permian Khuff Formation, which is made of shale and large conglomerates. There are fossilized marl, dolomite, sandstone, and gypsum in the upper part. A less significant discontinuous aquifer is the Khuff Formation.
3. Saq Sandstone, which is Cambrian to Ordovician in age. It depicts a regional aquifer system. The Saq Sandstone is above and frequently dipping east.
4. The Precambrian basement's Arabian shield complex.

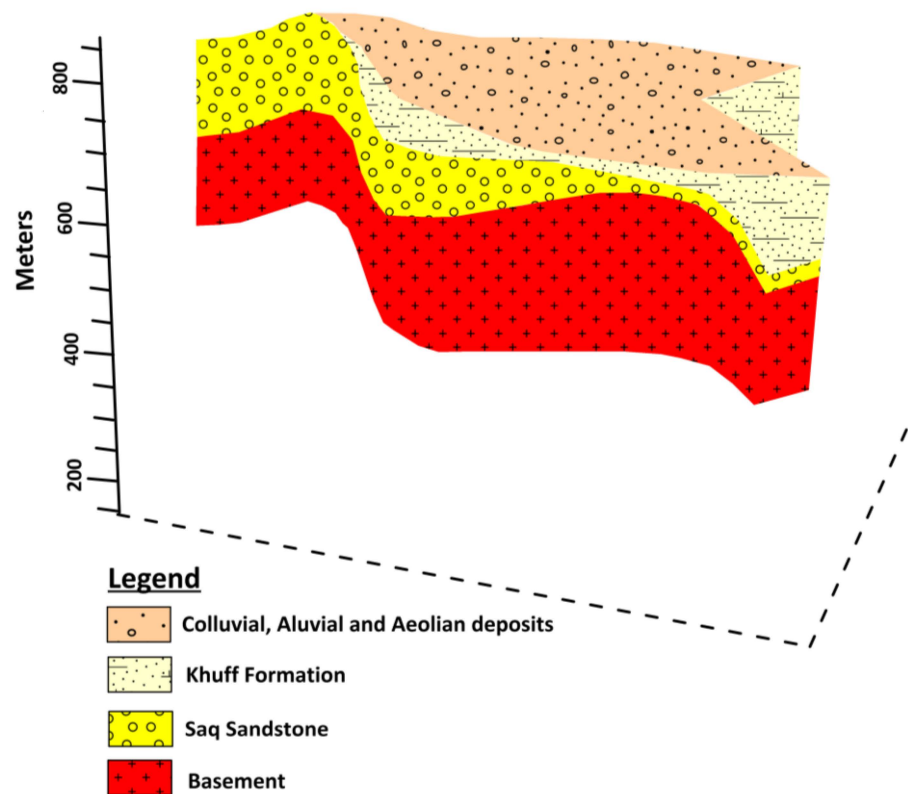


Figure 3. 3D subsurface stratigraphic units around the study area [75].

In addition to the subsurface geology, Figure 4 shows the surface geological map of the study area. Hydrogeologically, the Saq Sandstone is the main sedimentary aquifer system in the research area. It is a large aquifer that covers a large area in the region and holds a substantial quantity of groundwater (approximately 280 billion m³) [75]. Groundwater yields vary widely, typically from 50 to 100 L/s [75]. Except in cases when significant drops in water levels have caused a reversal of the groundwater hydraulic gradient, the natural flow direction of groundwater is northeast [75]. Precipitation, catchments downstream, and vertical infiltration from surface water systems replenish the Saq Sandstone. However, aquifer discharge occurs locally due to throughflow and irrigation bores in local production.

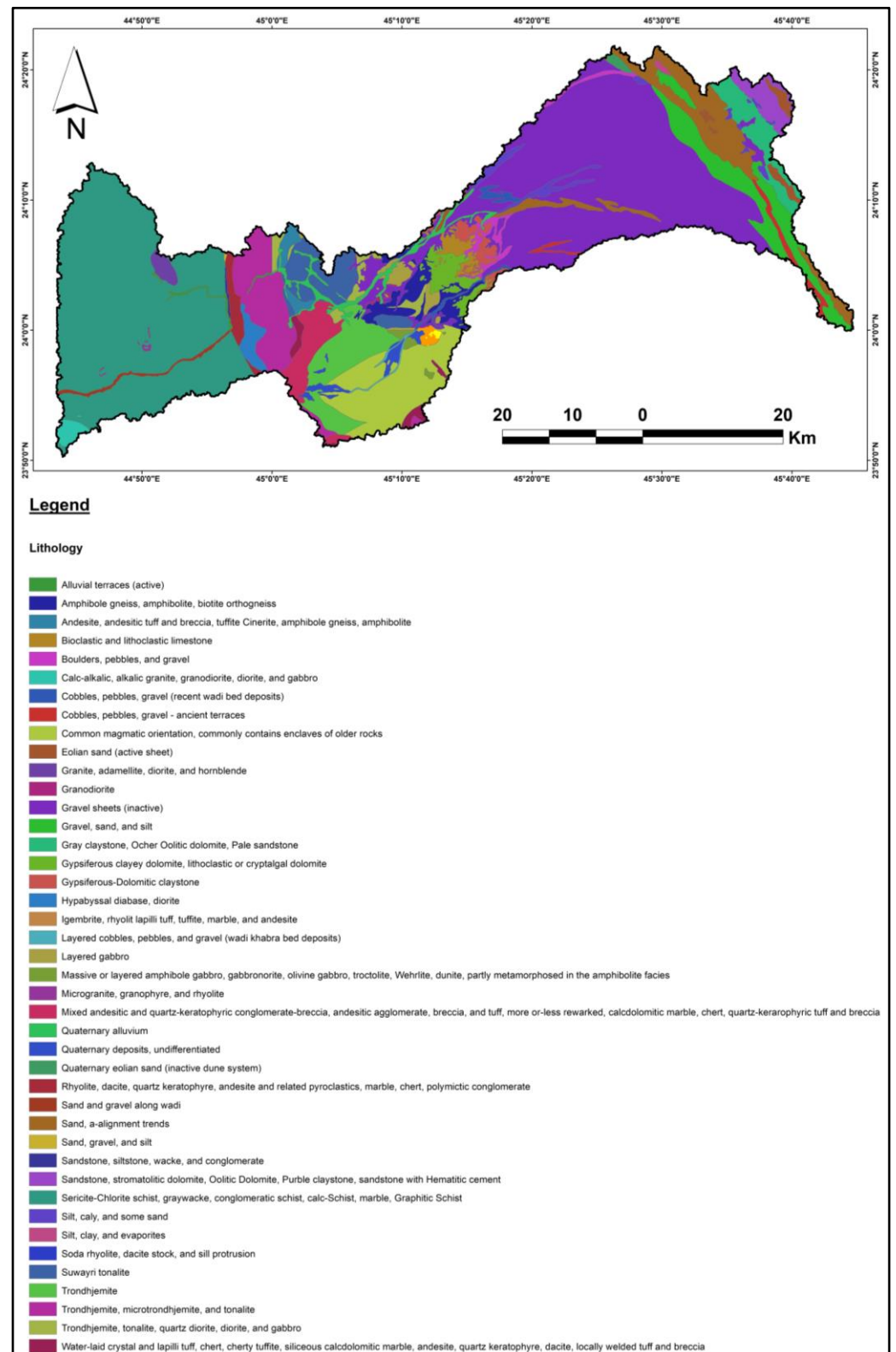


Figure 4. Geological map of the study area [77].

3. Materials and Methods

The present research used remote sensing imagery in conjunction with existing geological, hydrological, and other data to define possible recharge areas for water resources. Using a GIS-based technique, eleven significant thematic maps such as geology, elevation, slope, aspect, hill shade, flow direction, stream order, drainage density, lineaments,

lineaments density, and NDVI were combined (Figure 5). Remote sensing images were processed using ENVI v5.3 and ArcGIS v10.8 software. During the field investigation, information about groundwater was acquired, including groundwater well locations, the abundance and distribution of irrigated crops, and flow discharge.

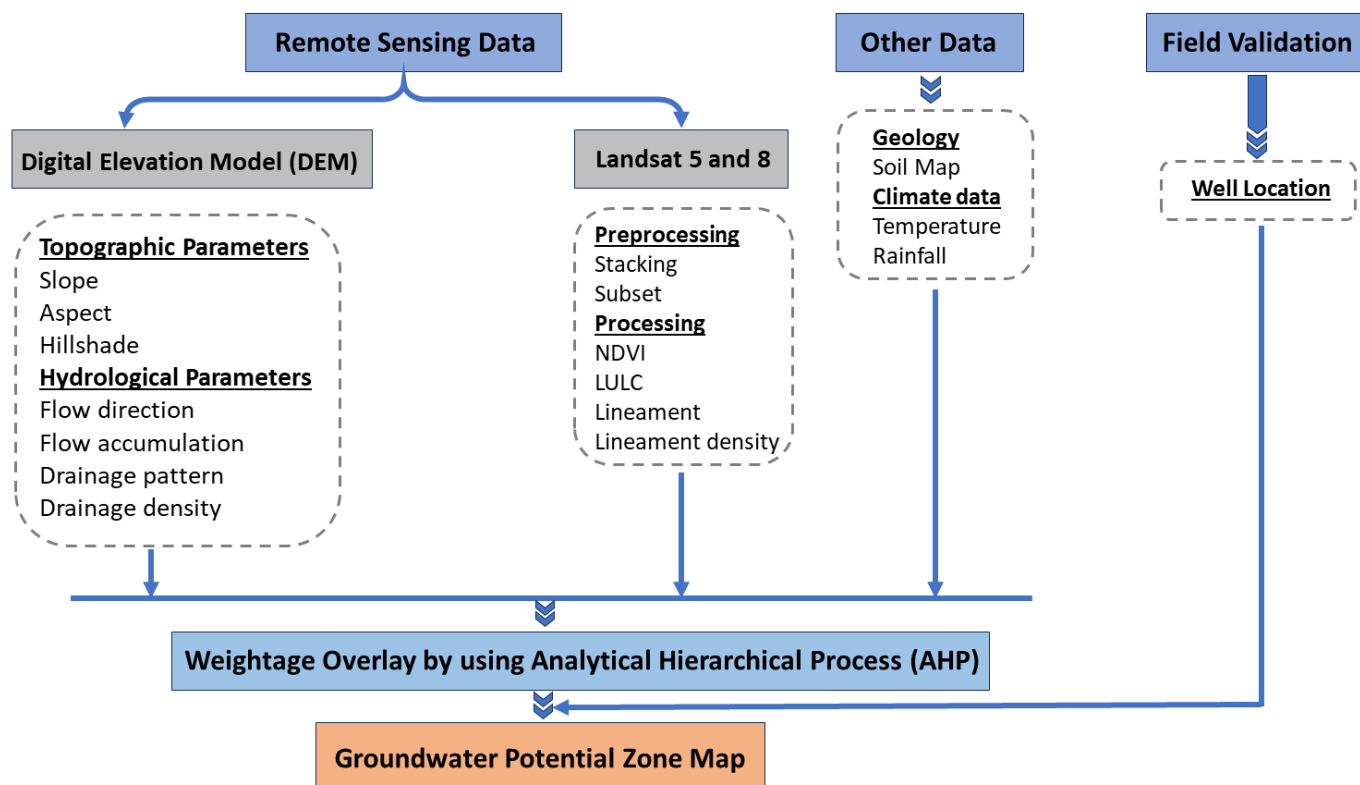


Figure 5. The flow chart illustrates the used methodology in the research.

In order to assess the topographical features, one of the Digital Elevation Models (DEMs) employed in this study was the Shuttle Radar Topography Mission (SRTM) data (30 m cell size). NASA provided SRTM DEM data (1 arc second). The Deterministic eight-neighbor (8D) technique was used to automatically generate a drainage system [78]. Then, using a GIS tool, this was transformed into a drainage density map. Furthermore, the fill-difference method was used to figure out the depressions to identify areas of water accumulation [79].

The operational land imager (OLI) and thermal infrared sensor (TIRS) are carried by Landsat 8, which was launched on 11 February 2013. The wavelength ranges considered in the study are shortwave infrared and visible and near-infrared. Image processing and enhancement techniques were used for a Landsat-8 OLI scene (path 166/row 44) that was acquired on 5 February 2023. Bands 1, 2, 3, 4, 5, and 7 were merged with a spatial resolution of 30 m and projected to WGS-84, UTM Zone 38 N. The vegetation cover that can be identified utilizing groundwater resources was shown by using data from Landsat 5 and 8. Consequently, we evaluated the vegetation areas by using the visible infrared bands and computed the normalized difference vegetation index (NDVI) by using the following equation for displaying the vegetation areas [80].

$$\text{NDVI} = (\text{NIR band} - \text{Red band}) / (\text{NIR band} + \text{Red band})$$

For the purpose of this study's NDVI change detection, we employed not only Landsat OLI but also a Landsat-5 scene (path 166/row 43), which was obtained on 25 August 2000 (bands 7, 4, and 2 in R, G, and B, respectively). A LULC map was also produced from the

landsat-8 OLI scene using a supervised classification method to identify the surface features within the study area. Using the maximum likelihood classifier (MLC) for parametric input data and field investigation, the resulting map is categorized into four classes based on supervised classification.

By integrating RS and GIS data applying the weighted overlay approach, the potential of groundwater resources was figured out. Proof of groundwater conditions was provided for every theme layer, including DEM, rainfall, geology, drainage density, slope, topography, soil, lineaments, flow accumulation, and flow direction maps. The rank of each layer—which is obtained by dividing the whole number of the layer rankings by the rank of each map—was converted to generate the GIS layer. The process of dividing each class's rank by the combined values of all the layer classes yields the capability values (CV_i). The groundwater potential zone map is created by multiplying these capability values by the relevant layer weight in each theme map. Following that, the potential occurrences are combined in a linear combination equation with the aid of the Raster Calculator tool. The steps provided are followed to complete the integration procedure.

$$GWP = \sum CV_i \times W_i \quad (1)$$

where GWP = groundwater potential, CV_i = capability value (weight of inter-map class), W_i = map weight.

Research on the integration of geographic information systems (GIS), remote sensing (RS), and GPS has grown popular in the fields of groundwater hydrology and environmental monitoring. Recent developments in RS, GIS, and GPS, and higher-level processing will make it easier to produce and handle a variety of data in a fast and economical manner. The use of RS and GIS, the necessity of integration models, hydrological modeling, and the outcome are all covered in this flowchart (Figure 5). We will be more capable of managing large data volumes and transferring knowledge about rapidly depleting societal resources if these issues have been resolved on a philosophical and technical level.

4. Results and Discussion

4.1. Topographical Parameters

Slope, aspect, and hillshade are examples of topographical factors that were extracted to achieve the target of the study.

4.1.1. Slope

Slope analysis is crucial for determining the best places for water infiltration since sites with low slopes have limited surface runoff and high percolating rates, whereas higher slopes encourage runoff and quick drainage of water [81]. According to the slope map, places with high slopes were found in the upstream section, particularly at the level of the basement in the center of the study area, whereas areas with low slopes were found in the downstream on the eastern side (Figure 6a). Runoff flows from the western side to the eastern side, and therefore the eastern side is generally more susceptible to groundwater recharge.

4.1.2. Aspect

The physical characteristics of soil structure, curved materials, and possible groundwater zones are all controlled by aspect, which reflects the vegetation, moisture retention, and inclination of rock bedding [82]. The present study reveals that the groundwater potential is positively weighted in the central and eastern regions of the study area, while the western portion of the study exhibits a negatively weighted groundwater potential zone map due to its more severe slope and gradient values (Figure 6b).

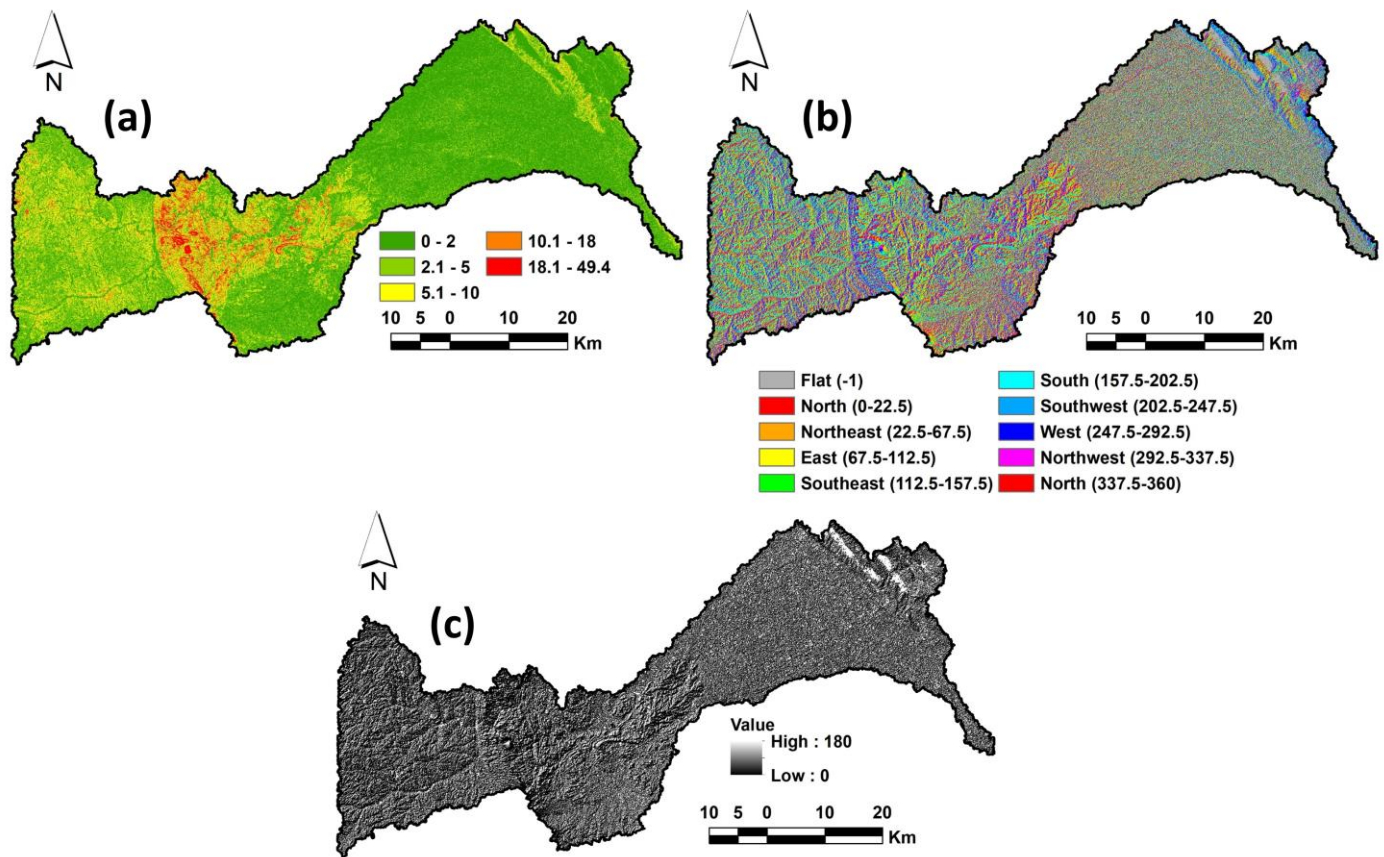


Figure 6. Topographical maps including: (a) Slope, (b) Aspect and (c) Hillshade.

4.1.3. Hillshade

Hillshade refers to a grayscale representation of the surface that uses the sun's relative position to determine how the relevant surface is colored. This feature uses azimuth and altitude data to define the sun's path. ArcGIS software 10.8's spatial analysis tool was used to extract the hillshade map. In the study area, the hillshade value varies from 0 to 180 (Figure 6c). Interpreting the entire basin area's steep terrain and surface topography depends heavily on this map.

4.2. Hydrological Parameters

4.2.1. Flow Direction

The network of streams was identified using a flow direction map, which depicts the movement of water along a surface that continually flows in the steepest downward direction. The river flows from the central to the eastern and northeastern regions, as shown by the flow direction map (Figure 7a). The relative proximity of the channel structure is indicated by the flow direction. Permeability factor and stream/flow direction are the opposite. More runoff in the direction of greatest flow indicates less water penetration below the surface (Table 1), and conversely [82].

Table 1. Layer map weights and their rank for groundwater recharge potential zones.

Factor	Weight	Category	Rank
Lineament Density (km/km²)			
0–0.01	27.6	Very Low	1
0.11–0.3		Low	2
0.31–0.5		Moderate	3
0.51–0.7		High	4
0.71–1.1		Very High	5
Slope			
0–2	12.3	Very High	5
2.1–5		High	4
5.1–10		Moderate	3
10.1–18		Low	2
18.1–49.4		Very Low	1
Topography			
645–733	8.7	Very High	5
733–815		High	4
815–899		Moderate	3
899–960		Low	2
960–1277		Very Low	1
Soil			
Sandy soil and gravel	8.3	Very High	4
Alluvial		High	3
Sandstone with limestone		Moderate	2
Hard rock		Low	1
Flow Direction			
<2	5.2	Very High	5
2–8		High	4
8–32		Moderate	3
32–64		Low	2
>64		Very Low	1
Flow Accumulation			
<2	5.7	Very High	5
2–3		High	4
3–5		Moderate	3
5–6		Low	2
>6		Very Low	1
LULC			
Vegetation	9.6	Moderate	2
Hard rocks		Low	1
Wadi deposits		Very High	4
Sedimentary rocks		High	3
Drainage Density (km/km²)			
7.8–51.8	8.9	Very High	5
51.81–95.93		High	4
95.93–140.06		Moderate	3
140.06–184.18		Low	2
184.18–228.31		Very Low	1
Rainfall (mm/Year)			
<20	13.6	Very Low	1
20–60		Low	2
60–90		Moderate	3
90–130		High	4
>130		Very High	5

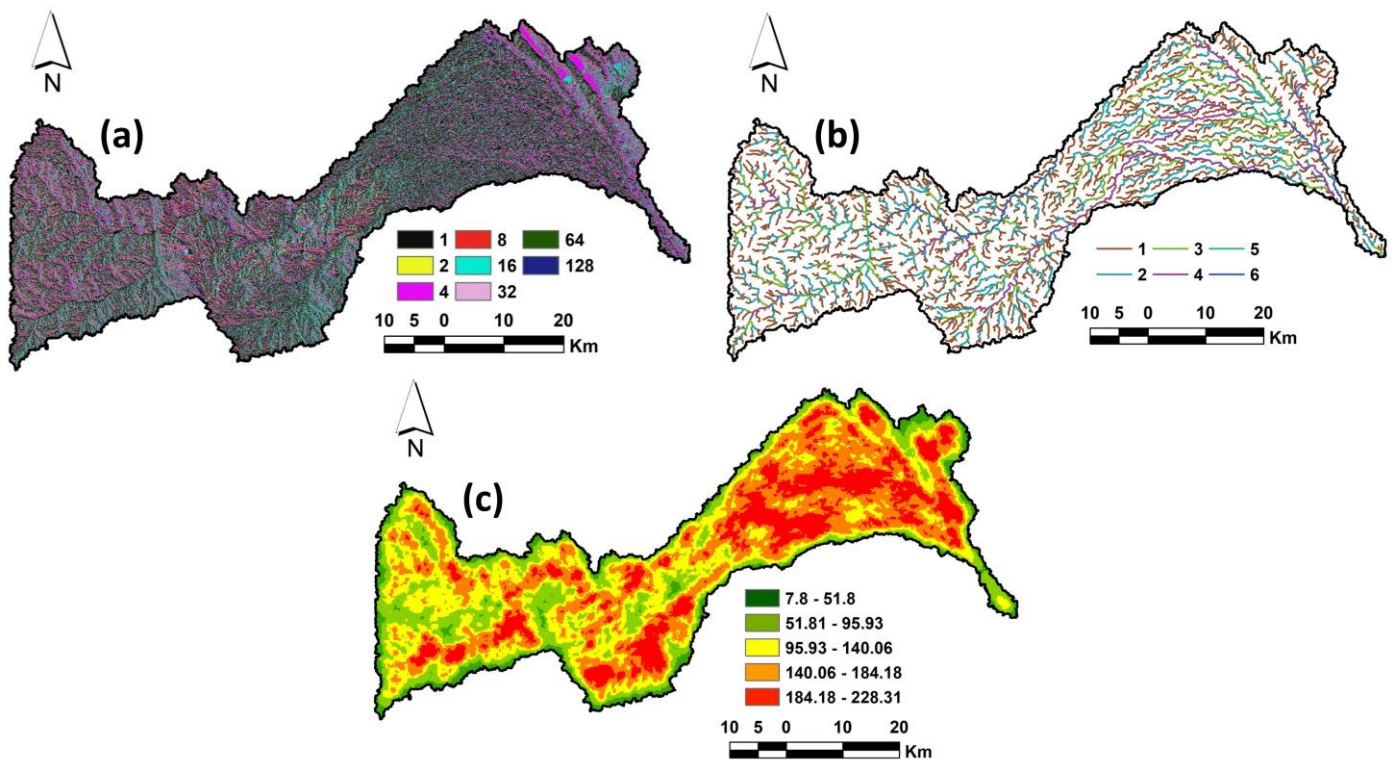


Figure 7. Hydrological maps including: (a) Flow direction, (b) stream orders and (c) Stream density.

4.2.2. Drainage Density

Furthermore, one of the main factors influencing the existence of groundwater in a particular basin is the drainage density [83]. It is calculated by dividing a basin's total area by the sum of all of its drainages [84]. Therefore, higher surface water runoff is accelerated by increased drainage density, but slower drainage density permits water to migrate more slowly and finally percolate into the ground surface [85,86]. Thus, the automatically generated stream networks in the study region were extracted, and the stream order was defined into six classes as a result (Figure 7b).

The uneven distribution of high to extremely high drainage densities in the northern, eastern, and southern regions of the study area suggests a limited groundwater potential. The medium to extremely low drainage densities in the remaining areas essentially encourage groundwater accumulation. The estimated drainage density in this investigation indicated a well-connected drainage system with extremely low to very high density, with values that varied from 7.8 to 228.3 lengths per unit area (Figure 7c). The Saaty model was utilized to rank and reclassify the drainage density categories based on their impact on groundwater supply. In comparison to low density drainage zones, which were rated higher with an average of 50%, high drainage density areas received a rating relatively lower, of 3%. According to investigations conducted in the coastal aquifer of eastern India, it was decided to impose a lower groundwater impact on an area with higher drainage density and larger effects on the lower drainage density [87].

4.2.3. Lineament

Lineaments on the surface of the Earth represent subsurface geological structures, including faults, fractures, and cracks with no visible fracture movement [88]. Because of their ability to allow groundwater distribution, they enhance secondary porosity, which makes them useful for locating possible groundwater regions [89]. A high-lineament density area may have significant groundwater potential (Table 1). Essential information on surface and subsurface fracture systems is provided by lineaments, which could influence groundwater flow and accumulation [88]. This has been used to distribute groundwater

resources and find potential sites for runoff water accumulation [79]. Promising areas for groundwater potential are indicated by higher lineament density, which also represent permeability zones [88]. ArcGIS's Spatial Analyst was used to digitize the lineaments (Figure 8a) of the basin from Landsat-8 and SRTM data and create a lineament density map. Five classes which represent 54.3, 13.8, 13.3, 12.3, and 6.16% of the lineament density map, respectively, are identified on the map (Figure 8b).

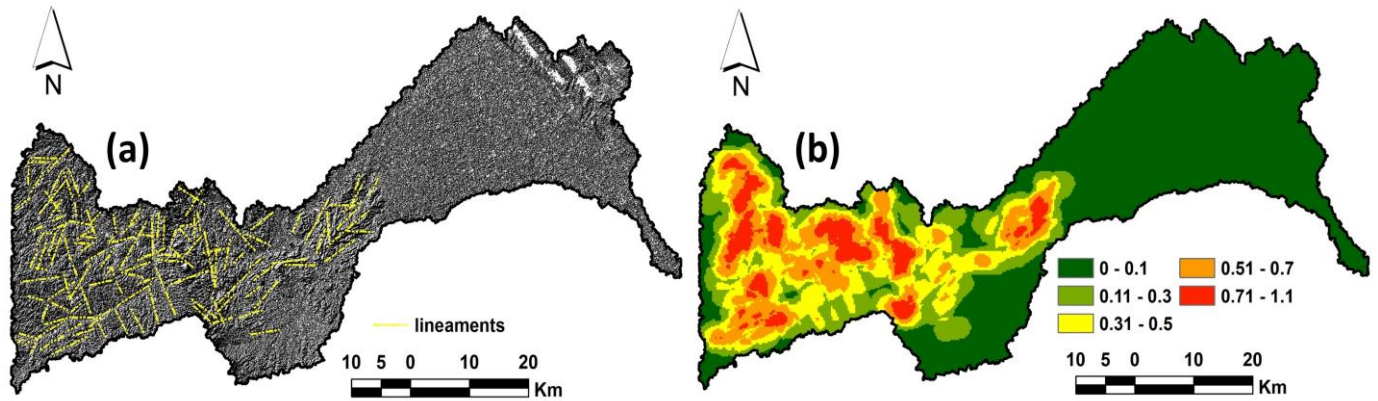


Figure 8. (a) The extracted lineament map (b) The lineament density map.

4.3. NDVI

One commonly utilized variable to assess groundwater potential zones is the NDVI [90] that represents the coverage and density of the vegetation. Landsat images (Figure 9a,b) were used to create the NDVI maps. The NDVI values range from -1 to 1 . Higher NDVI values indicate extensive vegetation. To figure out how the vegetation cover has changed between 2000 and 2023, the research area's NDVI result maps were extracted. The findings demonstrate that the vegetation cover expanded from 6 km^2 to 30 km^2 during a period of 23 years (Figure 9c,d). Generally, groundwater resources in the study area were used as a water source for vegetation in this period.

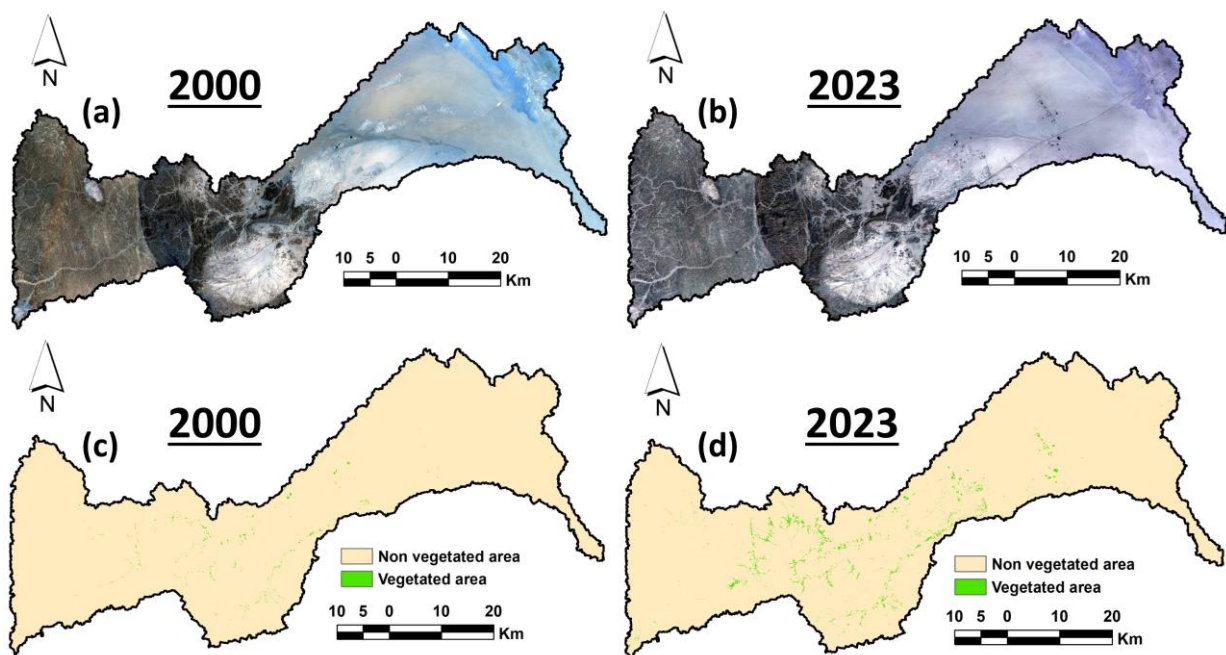


Figure 9. The temporal satellite images including: (a) Landsat-5 image for 2000 and (b) Landsat-8 image for 2023, (c) NDVI map for 2000, and (d) NDVI map for 2023.

4.4. LULC

The data were combined with a Landsat-8 OLI image for 2023, which helped classify land use and land cover (LULC). During field investigations, sample collections were gathered to generate reflectance values, or spectral signatures, for the supervised classification process, which determined the contents of the clusters, such as hard rocks, vegetation, wadi deposits, and sedimentary rocks. According to Figure 10, there are four primary classes in the LULC map. For roughly 40% of the overall area, there exist both hard rocks and sedimentary rocks. However, wadi deposits and vegetation cover make up 1.3% and 18.4% of the entire region, respectively. Using a confusion matrix with the ARCGIS program 10.8, the output map displays a 94% accuracy assessment rate.

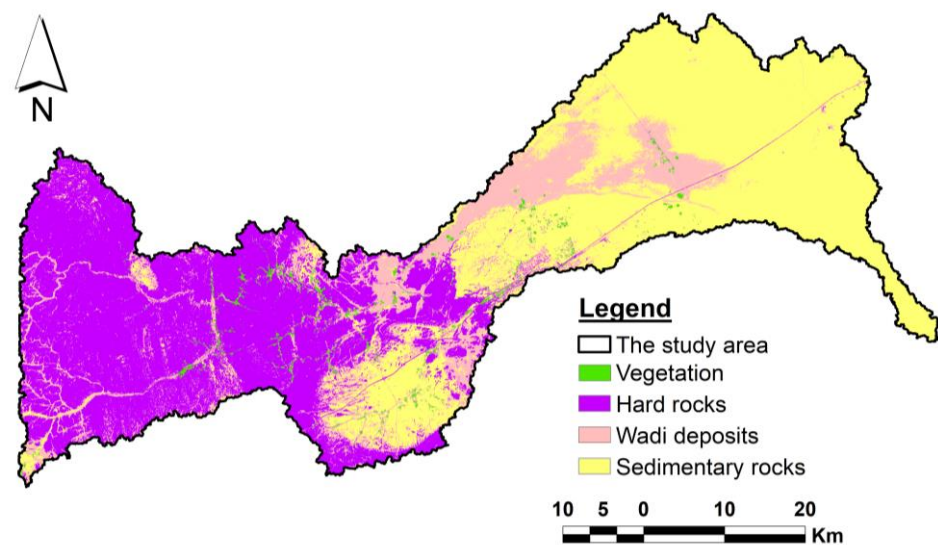


Figure 10. LULC map of the study area.

4.5. Groundwater Potential Zones

Prior to the integration of the thematic layers via the weighted overlay approach, consistency ratios were established for every thematic level and its subclasses. The results demonstrated the validity and reasonable consistency of the judgment matrices used in this investigation. As a result, the reclassified theme layers were integrated by utilizing the weighted overlay strategy, which depends on their weight, to create the groundwater potential map. The study region was classified, using the natural breaks/Jenks technique in the GIS platform, into five groups (i.e., very low, low, moderate, high, and very high groundwater potential zones) based on the values of the pixels (Figure 11). The majority filter in the GIS platform was used for additional processing of the map in order to reduce the pixel speckling.

The delineated map revealed discernible variations in the groundwater potential of the studied area. While areas of the district with subsurface hard rock are extremely vulnerable to a groundwater problem, approximately 7.9% of the region's distribution has very low groundwater potential. Regarding the possibility for groundwater, the map further designates 18.6% of the zone as semi-critical. However, it was discovered that there were still moderate, high, and very high groundwater potential zones in around 26.7%, 30%, and 16.8% of the study area, respectively. Because of the greater availability of runoff water and good groundwater recharge, a substantial potential for groundwater was found in several areas of the province along the flooded areas of the main rivers. As depicted in Figure 11, the southern and eastern regions of the examined basin have the highest concentration of streams, lineaments, and geological fractures, making them the most favorable locations for future drilling. These outcomes agree with the previous research [91,92].

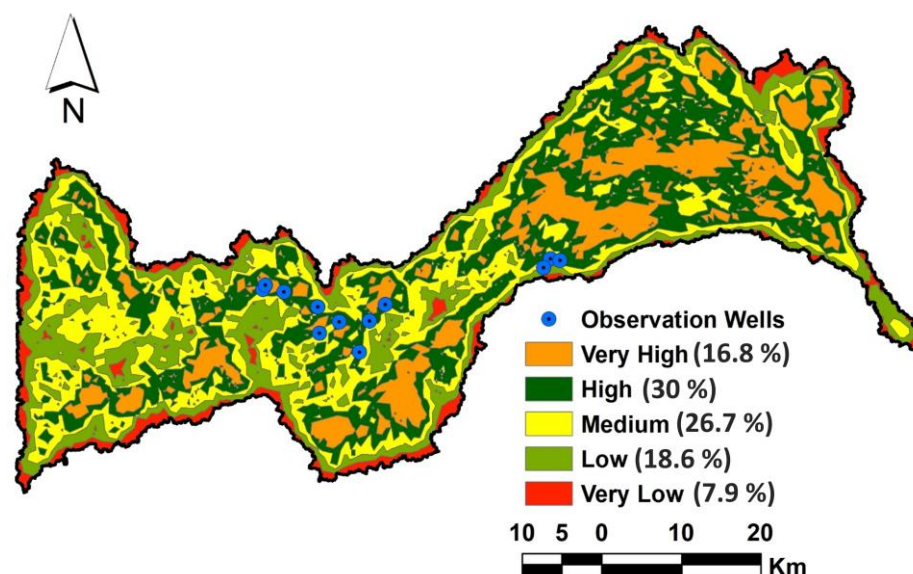


Figure 11. Groundwater potential recharge zones using AHP model and field data.

The research also included measurable cross-validation maps of groundwater prospect zones based on receiver operating characteristics (ROC). For a number of the variable's cut-off themes, the ROC display a true positive rate against an untrue positive rate; each concept on the path represents a sensitivity pair in relation to a threshold. Conversely, the area under the curve (AUC) determines the degree to which a factor can distinguish between the two sets of data. AUC values between 0.5 and 0.6 indicate poor forecast accuracy. Additionally, according to previous research [36,93], the 0.6–0.7, 0.7–0.8, 0.8–0.9, and 0.9–1 levels suggest very good, average, excellent, and good forecast accuracy, respectively. The AUC of the potential area map was 0.85, indicating that the results of the AHP approach were confirmed for good predictions. Thus, the current work reached a significantly higher accuracy rate with the largest number of appropriate theme maps by utilizing the AHP approach [94–96].

The identified potential zones can offer crucial methods for choosing new well regions in order to remove vigorous water resource management from the watershed zones. The application of a groundwater harvesting method may benefit from this result. Seeing the work's boundaries, creative potential, and limitations is fascinating. Although this study chose eleven theme layers, more accurate findings may have been obtained by including other data, such as hydro-geological and geomorphology maps (geomorphology and water level). The use of groundwater, water management, limited abstraction, sophisticated water framework, water awareness, alternative cropping techniques, and the conservation of home and industrial water are the main focuses of sustainable strategies. Long-term water management would benefit from the extraction of non-polluted groundwater. Because of the chosen methodology, the analysis has certain theoretical restrictions. AHP is additionally capable of suppressing errors. Groundwater zone rules are often significantly impacted by the volume of supply for agriculture and the amount of drinking water consumed; these issues were not included in this study. Nevertheless, the findings are precise and reasonable given the factors in the analysis method and prediction. The river basin's groundwater management can be improved with the use of the AHP data.

4.6. Field Validation

Field observations were used to validate the groundwater recharge potential map of the research area. To verify the combined results of RS and GIS, we collected data on the current wells (Table 2). The primary objectives of the field trip were to locate the wells and measure the depth and salinity of the water. Other information included soil type, topography, and surface geology (Figure 12a,b). These wells were drilled into the extremely

high and high potential zones in the central and eastern parts of the region. The wells were between 43 and 150 m deep (Figure 12c,d). The bottoms of these wells laid close to silt and clay beds, which act as barriers to deeper water infiltration. The salinity of groundwater varies from 1970 to 6600 mg/L. The groundwater's chemical makeup and suitability for irrigation were determined by a thorough investigation that we carried out before in previous work. Groundwater samples are appropriate for irrigation, according to the results [97]. The primary constituents of the surface soil sequence are gravel, sand, and silty sand. Consequently, the central and Eastern regions of the studied area (Figure 11) have been developed by local farmers, who irrigate many crops (Figure 12e,f) with good-quality groundwater. In addition, it was observed that groundwater is used for farming, and the majority of the wells in the research area have groundwater levels between 40 and 60 m deep. This demonstrates that rainfall, particularly during periods of precipitation, clearly replenishes the groundwater reservoir. This development aligns with the high potential area shown in the GW recharge potential map (Figure 11).

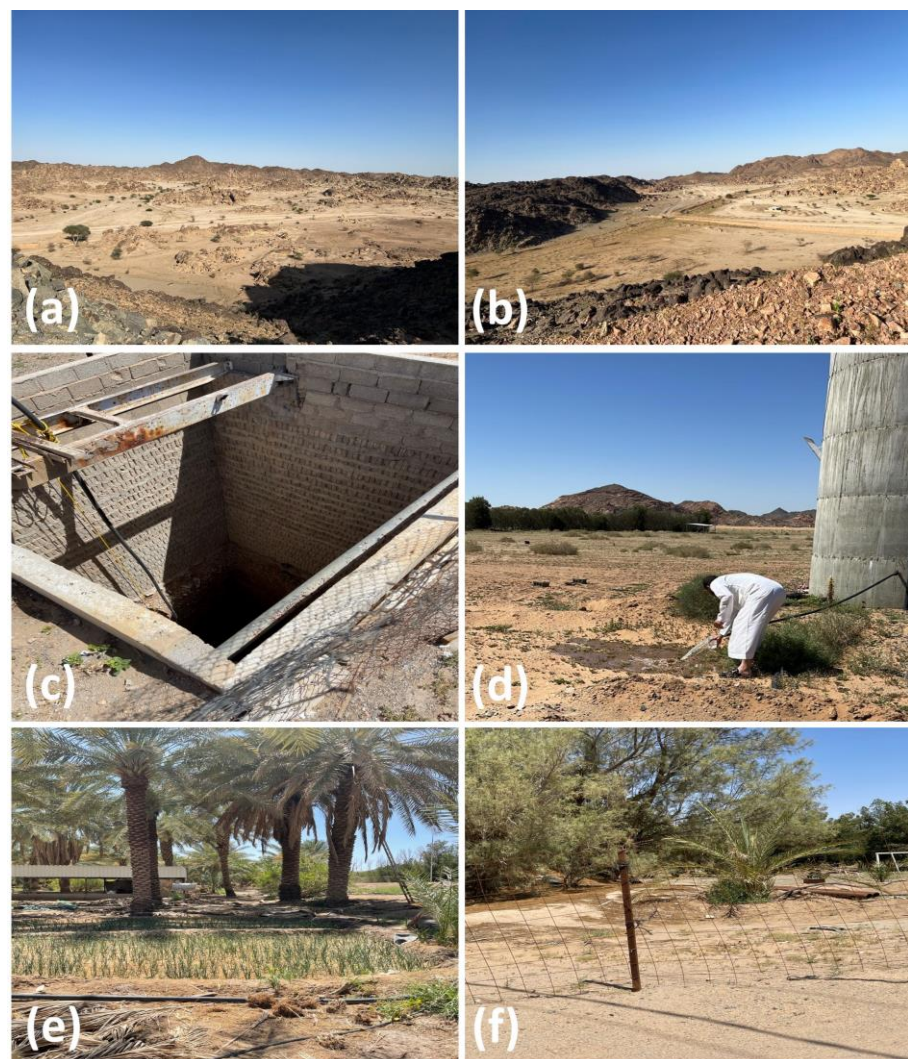


Figure 12. Field images showing: (a,b) The different geological and geomorphological units, (c,d) Water level observation from wells and (e,f) An example of farms in the study area.

Table 2. Wells dataset during the field validation.

X	Y	Elevation (m)	TDS (mg/L)	W.L (m)	Well Age (Years)
534,413.00 m E	2,665,349.00 m N	770	4405	110	14
533,274.00 m E	2,665,531.00 m N	777	4510	100	13
532,506.00 m E	2,664,425.00 m N	782	3720	150	12–15
514,308.00 m E	2,659,802.00 m N	822.5	3620	60	3
512,494.00 m E	2,657,740.00 m N	832.7	3290	60	3
511,331.00 m E	2,653,835.00 m N	871.8	2510	60	40
508,984.00 m E	2,657,588.00 m N	835.2	2520	60	7
506,704.00 m E	2,656,193.00 m N	862.1	5610	--	--
506,528.00 m E	2,659,460.00 m N	850.6	6180	57	more than 20
502,644.00 m E	2,661,355.00 m N	860.7	3370	43	more than 35
500,481.00 m E	2,662,234.00 m N	877.2	1970	50	1
500,206.00 m E	2,661,665.00 m N	878.3	6600	45	25–30

5. Conclusions

For sustainable development in arid and hyper-arid regions, groundwater is especially crucial as a water source. RS and GIS techniques are efficiently used to reveal, assess, and monitor exploratory data for water resources in different climatic conditions. RS and GIS techniques were used to study the SW Riyadh area in central Saudi Arabia. The primary objective was to locate possible recharge and groundwater potential zones. The geology, geomorphic, climatic, and hydrological characteristics are represented by twelve GIS conceptual layers that we combined in this instance. The lithology, elevation, slope, aspect, hillshade, drainage pattern, drainage density, NDVI, and lineament density are these different layers. Using an AHP overlay model based on geographic information systems, they were processed, normalized, and integrated.

The findings show the areas with potential for groundwater, which are divided into five categories: very high, high, moderate, low, and very low. These together represent 16.8, 30, 26.7, 18.6, and 7.9% of the total area. The model demonstrated good performance, as tested by field observation and the AUC (0.85). The locations that show promise are those that use artificial abstraction to supply groundwater. Overall, the GWPZ that is produced utilizing RS and GIS is very beneficial to decision makers and sustainability considerations. Additionally, this strategy can be used regionally and in locations with similar circumstances.

Author Contributions: Conceptualization, E.M.M.E.-B., H.M.A., M.H.S. and M.A.; methodology, E.M.M.E.-B., H.M.A., M.H.S. and M.A.; funding acquisition, E.M.M.E.-B. and H.M.A.; validation, E.M.M.E.-B. and H.M.A.; statical analysis, M.A.; writing—original draft preparation M.A., writing—review and editing, E.M.M.E.-B., H.M.A., M.H.S. and M.A. All authors have read and agreed to the published version of the manuscript.

Funding: This research received no external funding.

Data Availability Statement: Data are contained within the article.

Acknowledgments: Princess Nourah bint Abdulrahman University Researchers Supporting Project number (PNURSP2024R243), Princess Nourah bint Abdulrahman University, Riyadh, Saudi Arabia.

Conflicts of Interest: The authors declare no conflicts of interest.

References

1. Faramarzi, M.; Abbaspour, K.C.; Vaghefi, S.A.; Farzaneh, M.R.; Zehnder, A.J.B.; Srinivasan, R.; Yang, H. Modeling Impacts of Climate Change on Freshwater Availability in Africa. *J. Hydrol.* **2013**, *480*, 85–101. [\[CrossRef\]](#)
2. Abdelfattah, M.; Abdel-Aziz Abu-Bakr, H.; Aretouyap, Z.; Sheta, M.H.; Hassan, T.M.; Geriesh, M.H.; Shaheen, S.E.-D.; Alogayell, H.M.; M EL-Bana, E.M.; Gaber, A. Mapping the Impacts of the Anthropogenic Activities and Seawater Intrusion on the Shallow Coastal Aquifer of Port Said, Egypt. *Front. Earth Sci.* **2023**, *11*, 1204742. [\[CrossRef\]](#)

3. Shemsanga, C.; Muzuka, A.N.N.; Martz, L.; Komakech, H.; Mcharo, E. Indigenous Knowledge on Development and Management of Shallow Dug Wells of Dodoma Municipality in Tanzania. *Appl. Water Sci.* **2018**, *8*, 59. [[CrossRef](#)]
4. Gamal, G.; Hassan, T.M.; Gaber, A.; Abdelfattah, M. Groundwater Quality Assessment along the West of New Damietta Coastal City of Egypt Using an Integrated Geophysical and Hydrochemical Approaches. *Environ. Earth Sci.* **2023**, *82*, 107. [[CrossRef](#)]
5. Elbeih, S.F. An Overview of Integrated Remote Sensing and GIS for Groundwater Mapping in Egypt. *Ain Shams Eng. J.* **2015**, *6*, 1–15.
6. Kemper, K.E. Groundwater—From Development to Management. *Hydrogeol. J.* **2004**, *12*, 3–5. [[CrossRef](#)]
7. Xiao, R.; He, X.; Zhang, Y.; Ferreira, V.G.; Chang, L. Monitoring Groundwater Variations from Satellite Gravimetry and Hydrological Models: A Comparison with in-Situ Measurements in the Mid-Atlantic Region of the United States. *Remote Sens.* **2015**, *7*, 686–703. [[CrossRef](#)]
8. Molden, D. Water Responses to Urbanization. *Paddy Water Environ.* **2007**, *5*, 207–209. [[CrossRef](#)]
9. Altchenko, Y.; Villholth, K.G. Transboundary Aquifer Mapping and Management in Africa: A Harmonised Approach. *Hydrogeol. J.* **2013**, *21*, 1497–1517. [[CrossRef](#)]
10. Owolabi, S.T.; Madi, K.; Kalumba, A.M.; Alemaw, B.F. Assessment of Recession Flow Variability and the Surficial Lithology Impact: A Case Study of Buffalo River Catchment, Eastern Cape, South Africa. *Environ. Earth Sci.* **2020**, *79*, 187. [[CrossRef](#)]
11. Barlow, P.M.; Leake, S.A. *Streamflow Depletion by Wells: Understanding and Managing the Effects of Groundwater Pumping on Streamflow*; US Geological Survey: Reston, VA, USA, 2012; Volume 1376.
12. Barker, J.A. A Generalized Radial Flow Model for Hydraulic Tests in Fractured Rock. *Water Resour. Res.* **1988**, *24*, 1796–1804.
13. Chowdhury, A.; Jha, M.K.; Chowdary, V.M. Delineation of Groundwater Recharge Zones and Identification of Artificial Recharge Sites in West Medinipur District, West Bengal, Using RS, GIS and MCDM Techniques. *Environ. Earth Sci.* **2010**, *59*, 1209–1222. [[CrossRef](#)]
14. Meshram, K.S.; Tripathi, M.P.; Mukharjee, A.P. Effect of Artificial Recharge Structures on Ground Water Availability in Semi-Critical Area in Chhattisgarh. Ph.D. Thesis, Indira Gandhi KrishiVishwavidyalaya, Raipur, India, 2010.
15. Samson, S.; Elangovan, K. Delineation of Groundwater Recharge Potential Zones in Namakkal District, Tamilnadu, India Using Remote Sensing and GIS. *J. Indian Soc. Remote Sens.* **2015**, *43*, 769–778. [[CrossRef](#)]
16. Taheri, A.; Zare, M. Groundwater Artificial Recharge Assessment in Kangavar Basin, a Semi-Arid Region in the Western Part of Iran. *Afr. J. Agric. Res.* **2011**, *6*, 4370–4384.
17. Murthy, K.S.R. Ground Water Potential in a Semi-Arid Region of Andhra Pradesh—a Geographical Information System Approach. *Int. J. Remote Sens.* **2000**, *21*, 1867–1884. [[CrossRef](#)]
18. Srinivasa Rao, Y.; Reddy, T.; Nayudu, P. Groundwater Targeting in a Hard-Rock Terrain Using Fracture-Pattern Modeling, Niva River Basin, Andhra Pradesh, India. *Hydrogeol. J.* **2000**, *8*, 494–502.
19. Jaiswal, R.K.; Mukherjee, S.; Krishnamurthy, J.; Saxena, R. Role of Remote Sensing and GIS Techniques for Generation of Groundwater Prospect Zones towards Rural Development—An Approach. *Int. J. Remote Sens.* **2003**, *24*, 993–1008. [[CrossRef](#)]
20. Srivastava, P.K.; Bhattacharya, A.K. Groundwater Assessment through an Integrated Approach Using Remote Sensing, GIS and Resistivity Techniques: A Case Study from a Hard Rock Terrain. *Int. J. Remote Sens.* **2006**, *27*, 4599–4620. [[CrossRef](#)]
21. Dinesh Kumar, P.K.; Gopinath, G.; Seralathan, P. Application of Remote Sensing and GIS for the Demarcation of Groundwater Potential Zones of a River Basin in Kerala, Southwest Coast of India. *Int. J. Remote Sens.* **2007**, *28*, 5583–5601. [[CrossRef](#)]
22. Mondal, N.C.; Das, S.N.; Singh, V.S. Integrated Approach for Identification of Potential Groundwater Zones in Seethanagaram Mandal of Vizianagaram District, Andhra Pradesh, India. *J. Earth Syst. Sci.* **2008**, *117*, 133–144. [[CrossRef](#)]
23. Chowdhury, A.; Jha, M.K.; Chowdary, V.M.; Mal, B.C. Integrated Remote Sensing and GIS-based Approach for Assessing Groundwater Potential in West Medinipur District, West Bengal, India. *Int. J. Remote Sens.* **2009**, *30*, 231–250. [[CrossRef](#)]
24. Dhakate, R.; Chowdhary, D.K.; Gurunadha Rao, V.V.S.; Tiwary, R.K.; Sinha, A. Geophysical and Geomorphological Approach for Locating Groundwater Potential Zones in Sukinda Chromite Mining Area. *Environ. Earth Sci.* **2012**, *66*, 2311–2325. [[CrossRef](#)]
25. Nag, S.K.; Ghosh, P. Delineation of Groundwater Potential Zone in Chhatna Block, Bankura District, West Bengal, India Using Remote Sensing and GIS Techniques. *Environ. Earth Sci.* **2013**, *70*, 2115–2127. [[CrossRef](#)]
26. Balakrishna; Balaji Shrikant Maury, S.; Narshimulu, G. Ground Water Potential in Fractured Aquifers of Ophiolite Formations, Port Blair, South Andaman Islands Using Electrical Resistivity Tomography (ERT) and Vertical Electrical Sounding (VES). *J. Geol. Soc. India* **2014**, *83*, 393–402.
27. Sonkamble, S.; Satishkumar, V.; Amarender, B.; Sethurama, S. Combined Ground-Penetrating Radar (GPR) and Electrical Resistivity Applications Exploring Groundwater Potential Zones in Granitic Terrain. *Arab. J. Geosci.* **2014**, *7*, 3109–3117. [[CrossRef](#)]
28. Al-Abadi, A.M. Groundwater Potential Mapping at Northeastern Wasit and Missan Governorates, Iraq Using a Data-Driven Weights of Evidence Technique in Framework of GIS. *Environ. Earth Sci.* **2015**, *74*, 1109–1124. [[CrossRef](#)]
29. Mezni, I.; Chihi, H.; Hammami, M.A.; Gabtni, H.; Baba Sy, M. Regionalization of Natural Recharge Zones Using Analytical Hierarchy Process in an Arid Hydrologic Basin: A Contribution for Managed Aquifer Recharge. *Nat. Resour. Res.* **2022**, *31*, 867–895. [[CrossRef](#)]
30. Khan, M.Y.A.; ElKashouty, M.; Tian, F. Mapping Groundwater Potential Zones Using Analytical Hierarchical Process and Multicriteria Evaluation in the Central Eastern Desert, Egypt. *Water* **2022**, *14*, 1041. [[CrossRef](#)]
31. Khan, M.Y.A.; ElKashouty, M.; Subyani, A.M.; Tian, F.; Gusti, W. GIS and RS Intelligence in Delineating the Groundwater Potential Zones in Arid Regions: A Case Study of Southern Aseer, Southwestern Saudi Arabia. *Appl. Water Sci.* **2022**, *12*, 3. [[CrossRef](#)]

32. Pradhan, R.M.; Guru, B.; Pradhan, B.; Biswal, T.K. Integrated Multi-Criteria Analysis for Groundwater Potential Mapping in Precambrian Hard Rock Terranes (North Gujarat), India. *Hydrol. Sci. J.* **2021**, *66*, 961–978. [[CrossRef](#)]
33. Diriba, D.; Karuppanan, S.; Takele, T.; Husein, M. Delineation of Groundwater Potential Zonation Using Geoinformatics and AHP Techniques with Remote Sensing Data. *Heliyon* **2024**, *10*, e25532. [[CrossRef](#)] [[PubMed](#)]
34. Feujio, D.H.A.; Aretouyap, Z.; Tchato, S.C.; Legrand, C.N.I.I.; Djomdi, E.; Madadjeu, N.N.; Nguimgo, C.N.; Kpoumie, A.N. Application of Analytical Hierarchy Process to Assess Groundwater Potential for a Sustainable Management in the Menoua Division. *Heliyon* **2024**, *10*, e24310. [[CrossRef](#)] [[PubMed](#)]
35. Arulbalaji, P.; Padmalal, D.; Sreelash, K. GIS and AHP Techniques Based Delineation of Groundwater Potential Zones: A Case Study from Southern Western Ghats, India. *Sci. Rep.* **2019**, *9*, 2082. [[CrossRef](#)] [[PubMed](#)]
36. Ajay Kumar, V.; Mondal, N.C.; Ahmed, S. Identification of Groundwater Potential Zones Using RS, GIS and AHP Techniques: A Case Study in a Part of Deccan Volcanic Province (DVP), Maharashtra, India. *J. Indian Soc. Remote Sens.* **2020**, *48*, 497–511. [[CrossRef](#)]
37. Yariyan, P.; Avand, M.; Omidvar, E.; Pham, Q.B.; Linh, N.T.T.; Tiefenbacher, J.P. Optimization of Statistical and Machine Learning Hybrid Models for Groundwater Potential Mapping. *Geocarto Int.* **2022**, *37*, 3877–3911. [[CrossRef](#)]
38. Sun, T.; Cheng, W.; Abdelkareem, M.; Al-Arifi, N. Mapping Prospective Areas of Water Resources and Monitoring Land Use/Land Cover Changes in an Arid Region Using Remote Sensing and GIS Techniques. *Water* **2022**, *14*, 2435. [[CrossRef](#)]
39. Abdelkareem, M.; El-Baz, F.; Askalany, M.; Akawy, A.; Ghoneim, E. Groundwater Prospect Map of Egypt's Qena Valley Using Data Fusion. *Int. J. Image Data Fusion* **2012**, *3*, 169–189. [[CrossRef](#)]
40. Melese, T.; Belay, T. Groundwater Potential Zone Mapping Using Analytical Hierarchy Process and GIS in Muga Watershed, Abay Basin, Ethiopia. *Glob. Challenges* **2022**, *6*, 2100068. [[CrossRef](#)]
41. Priya, U.; Iqbal, M.A.; Salam, M.A.; Nur-E-Alam, M.; Uddin, M.F.; Islam, A.R.M.T.; Sarkar, S.K.; Imran, S.I.; Rak, A.E. Sustainable Groundwater Potential Zoning with Integrating GIS, Remote Sensing, and AHP Model: A Case from North-Central Bangladesh. *Sustainability* **2022**, *14*, 5640. [[CrossRef](#)]
42. Pourtaghi, Z.S.; Pourghasemi, H.R. GIS-Based Groundwater Spring Potential Assessment and Mapping in the Birjand Township, Southern Khorasan Province, Iran. *Hydrogeol. J.* **2014**, *22*, 643–662. [[CrossRef](#)]
43. Naghibi, S.A.; Pourghasemi, H.R.; Dixon, B. GIS-Based Groundwater Potential Mapping Using Boosted Regression Tree, Classification and Regression Tree, and Random Forest Machine Learning Models in Iran. *Environ. Monit. Assess.* **2016**, *188*, 1–27. [[CrossRef](#)] [[PubMed](#)]
44. Guru, B.; Seshan, K.; Bera, S. Frequency Ratio Model for Groundwater Potential Mapping and Its Sustainable Management in Cold Desert, India. *J. King Saud Univ.* **2017**, *29*, 333–347. [[CrossRef](#)]
45. Machiwal, D.; Jha, M.K.; Mal, B.C. Assessment of Groundwater Potential in a Semi-Arid Region of India Using Remote Sensing, GIS and MCDM Techniques. *Water Resour. Manag.* **2011**, *25*, 1359–1386. [[CrossRef](#)]
46. Ishizaka, A.; Labib, A. Review of the Main Developments in the Analytic Hierarchy Process. *Expert Syst. Appl.* **2011**, *38*, 14336–14345. [[CrossRef](#)]
47. Maity, D.K.; Mandal, S. Identification of Groundwater Potential Zones of the Kumari River Basin, India: An RS & GIS Based Semi-Quantitative Approach. *Environ. Dev. Sustain.* **2019**, *21*, 1013–1034.
48. Saaty, T.L. A Scaling Method for Priorities in Hierarchical Structures. *J. Math. Psychol.* **1977**, *15*, 234–281. [[CrossRef](#)]
49. Saaty, T.L. *The Analytic Hierarchy Process: Planning, Priority Setting, Resource Allocation*; McGraw-Hill International: New York, NY, USA, 1980.
50. Baghel, S.; Tripathi, M.P.; Khalkho, D.; Al-Ansari, N.; Kumar, A.; Elbeltagi, A. Delineation of Suitable Sites for Groundwater Recharge Based on Groundwater Potential with RS, GIS, and AHP Approach for Mand Catchment of Mahanadi Basin. *Sci. Rep.* **2023**, *13*, 9860. [[CrossRef](#)]
51. Chenini, I.; Ben, M.A.; El May, M. Groundwater Recharge Zone Mapping Using GIS-Based Multi-Criteria Analysis: A Case Study in Central Tunisia (Maknassy Basin). *Water Resour. Manag.* **2010**, *24*, 921–939. [[CrossRef](#)]
52. Gumma, M.K.; Pavelic, P. Mapping of Groundwater Potential Zones across Ghana Using Remote Sensing, Geographic Information Systems, and Spatial Modeling. *Environ. Monit. Assess.* **2013**, *185*, 3561–3579. [[CrossRef](#)]
53. Sener, E.; Davraz, A.; Ozcelik, M. An Integration of GIS and Remote Sensing in Groundwater Investigations: A Case Study in Burdur, Turkey. *Hydrogeol. J.* **2005**, *13*, 826–834. [[CrossRef](#)]
54. Abdalla, F. Mapping of Groundwater Prospective Zones Using Remote Sensing and GIS Techniques: A Case Study from the Central Eastern Desert, Egypt. *J. Afr. Earth Sci.* **2012**, *70*, 8–17. [[CrossRef](#)]
55. Gaber, A.; Mohamed, A.K.; ElGalladi, A.; Abdelkareem, M.; Beshr, A.M.; Koch, M. Mapping the Groundwater Potentiality of West Qena Area, Egypt, Using Integrated Remote Sensing and Hydro-Geophysical Techniques. *Remote Sens.* **2020**, *12*, 1559. [[CrossRef](#)]
56. Abdekareem, M.; Abdalla, F.; Al-Arifi, N.; Bamousa, A.O.; El-Baz, F. Using Remote Sensing and GIS-Based Frequency Ratio Technique for Revealing Groundwater Prospective Areas at Wadi Al Hamdh Watershed, Saudi Arabia. *Water* **2023**, *15*, 1154. [[CrossRef](#)]
57. Rahmati, O.; Nazari Samani, A.; Mahdavi, M.; Pourghasemi, H.R.; Zeinivand, H. Groundwater Potential Mapping at Kurdistan Region of Iran Using Analytic Hierarchy Process and GIS. *Arab. J. Geosci.* **2015**, *8*, 7059–7071. [[CrossRef](#)]

58. Roy, S.; Hazra, S.; Chanda, A.; Das, S. Assessment of Groundwater Potential Zones Using Multi-Criteria Decision-Making Technique: A Micro-Level Case Study from Red and Lateritic Zone (RLZ) of West Bengal, India. *Sustain. Water Resour. Manag.* **2020**, *6*, 1–14. [[CrossRef](#)]
59. Solomon, S.; Ghebreab, W. Hard-Rock Hydrotectonics Using Geographic Information Systems in the Central Highlands of Eritrea: Implications for Groundwater Exploration. *J. Hydrol.* **2008**, *349*, 147–155. [[CrossRef](#)]
60. Lubang Nobert, J.B.; Mtaló, E.G. Integrated Remote Sensing and GIS Techniques for Groundwater Exploration in Semi-Arid Region: A Case of Karamoja Region-Uganda. *Tanzan. J. Eng. Technol.* **2008**, *2*, 31–42.
61. Kuria, D.N.; Gachari, M.K.; Macharia, M.W.; Mungai, E. Mapping Groundwater Potential in Kitui District, Kenya Using Geospatial Technologies. *Int. J. Water Resour. Environ. Eng.* **2012**, *4*, 15–22.
62. Konkul, J.; Rojborwornwittaya, W.; Chotpantararat, S. Hydrogeologic Characteristics and Groundwater Potentiality Mapping Using Potential Surface Analysis in the Huay Sai Area, Phetchaburi Province, Thailand. *Geosci. J.* **2014**, *18*, 89–103. [[CrossRef](#)]
63. Li, Y.; Abdelkareem, M.; Al-Arifi, N. Mapping Potential Water Resource Areas Using GIS-Based Frequency Ratio and Evidential Belief Function. *Water* **2023**, *15*, 480. [[CrossRef](#)]
64. Al-Omran, A.M.; Aly, A.A.; Al-Wabel, M.I.; Sallam, A.S.; Al-Shayaa, M.S. Hydrochemical Characterization of Groundwater under Agricultural Land in Arid Environment: A Case Study of Al-Kharj, Saudi Arabia. *Arab. J. Geosci.* **2016**, *9*, 68. [[CrossRef](#)]
65. Mahmoud, S.H.; Alazba, A.A. The Potential of in Situ Rainwater Harvesting in Arid Regions: Developing a Methodology to Identify Suitable Areas Using GIS-Based Decision Support System. *Arab. J. Geosci.* **2015**, *8*, 5167–5179. [[CrossRef](#)]
66. Mahmoud, S.H.; Alazba, A.A. Identification of Potential Sites for Groundwater Recharge Using a GIS-Based Decision Support System in Jazan Region-Saudi Arabia. *Water Resour. Manag.* **2014**, *28*, 3319–3340. [[CrossRef](#)]
67. Al-Rashed, M.F.; Sherif, M.M. Water Resources in the GCC Countries: An Overview. *Water Resour. Manag.* **2000**, *14*, 59–75. [[CrossRef](#)]
68. Khouri, J.; Agha, W.; Al-Deroubi, A. Water Resources in the Arab World and Future Perspectives. In Proceedings of the Symposium on Water Resources and Uses in the Arab World, Kuwait, 1986.
69. Ukayli, M.A.; Husain, T. Comparative Evaluation of Surface Water Availability, Wastewater Reuse and Desalination in Saudi Arabia. *Water Int.* **1988**, *13*, 218–225. [[CrossRef](#)]
70. Abdulrazzak, M.J. Water Supplies versus Demand in Countries of Arabian Peninsula. *J. Water Resour. Plan. Manag.* **1995**, *121*, 227–234. [[CrossRef](#)]
71. Alghamdi, A.G.; Aly, A.A.; Aldhumri, S.A.; Al-Barakaha, F.N. Hydrochemical and Quality Assessment of Groundwater Resources in Al-Madinah City, Western Saudi Arabia. *Sustainability* **2020**, *12*, 3106. [[CrossRef](#)]
72. Saud, A.G.; Abdullah, S.A. Water Resources and Reuse in Al-Madinah. In Proceedings of the International Conference on Water Conservation in Arid Regions (ICWCAR'09), Water Research Center-King Abdulaziz University, Jeddah, Saudi Arabia, 12–14 October 2009; pp. 12–14.
73. Ali, I.; Hasan, M.A.; Alharbi, O.M.L. Toxic Metal Ions Contamination in the Groundwater, Kingdom of Saudi Arabia. *J. Taibah Univ. Sci.* **2020**, *14*, 1571–1579. [[CrossRef](#)]
74. MOEP (The Ministry of Economy and Planning). *The Ninth Development Plan (2010–2014)*; MOEP (The Ministry of Economy and Planning): Riyadh, Saudi Arabia, 2014.
75. Yihdego, Y.; Drury, L. Mine Water Supply Assessment and Evaluation of the System Response to the Designed Demand in a Desert Region, Central Saudi Arabia. *Environ. Monit. Assess.* **2016**, *188*, 619. [[CrossRef](#)]
76. Available online: <https://www.worldweatheronline.com/riyadh-weather-averages/ar-riyadh/sa.aspx> (accessed on 22 November 2023).
77. Available online: <https://ngp.sgs.gov.sa/> (accessed on 3 December 2023).
78. O'Callaghan, J.F.; Mark, D.M. The Extraction of Drainage Networks from Digital Elevation Data. *Comput. Vis. Graph. Image Process.* **1984**, *28*, 323–344. [[CrossRef](#)]
79. Zhu, Q.; Abdelkareem, M. Mapping Groundwater Potential Zones Using a Knowledge-Driven Approach and GIS Analysis. *Water* **2021**, *13*, 579. [[CrossRef](#)]
80. Abdelkareem, M.; Abdalla, F. Revealing Potential Areas of Water Resources Using Integrated Remote-Sensing Data and GIS-Based Analytical Hierarchy Process. *Geocarto Int.* **2021**, *37*, 8672–8696. [[CrossRef](#)]
81. Mogaji, K.A.; Lim, H.S.; Abdullah, K. Regional Prediction of Groundwater Potential Mapping in a Multifaceted Geology Terrain Using GIS-Based Dempster–Shafer Model. *Arab. J. Geosci.* **2015**, *8*, 3235–3258. [[CrossRef](#)]
82. Pande, C.B.; Moharir, K.N.; Panneerselvam, B.; Singh, S.K.; Elbeltagi, A.; Pham, Q.B.; Varade, A.M.; Rajesh, J. Delineation of Groundwater Potential Zones for Sustainable Development and Planning Using Analytical Hierarchy Process (AHP), and MIF Techniques. *Appl. Water Sci.* **2021**, *11*, 186. [[CrossRef](#)]
83. Megahed, H.A.; Farrag, A.E.-H.A.; Mohamed, A.A.; D'Antonio, P.; Scopa, A.; AbdelRahman, M.A.E. Groundwater Recharge Potentiality Mapping in Wadi Qena, Eastern Desert Basins of Egypt for Sustainable Agriculture Base Using Geomatics Approaches. *Hydrology* **2023**, *10*, 237. [[CrossRef](#)]
84. Tolche, A.D. Groundwater Potential Mapping Using Geospatial Techniques: A Case Study of Dhungeta-Ramis Sub-Basin, Ethiopia. *Geol. Ecol. Landsc.* **2020**, *5*, 65–80. [[CrossRef](#)]
85. Biswas, S.; Mukhopadhyay, B.P.; Bera, A. Delineating Groundwater Potential Zones of Agriculture Dominated Landscapes Using GIS Based AHP Techniques: A Case Study from Uttar Dinajpur District, West Bengal. *Environ. Earth Sci.* **2020**, *79*, 302. [[CrossRef](#)]

86. Magesh, N.S.; Chandrasekar, N.; Soundranayagam, J.P. Delineation of Groundwater Potential Zones in Theni District, Tamil Nadu, Using Remote Sensing, GIS and MIF Techniques. *Geosci. Front.* **2012**, *3*, 189–196. [[CrossRef](#)]
87. Mandal, U.; Sahoo, S.; Munusamy, S.B.; Dhar, A.; Panda, S.N.; Kar, A.; Mishra, P.K. Delineation of Groundwater Potential Zones of Coastal Groundwater Basin Using Multi-Criteria Decision Making Technique. *Water Resour. Manag.* **2016**, *30*, 4293–4310. [[CrossRef](#)]
88. Abdelkareem, M.; El-Baz, F. Remote Sensing of Paleodrainage Systems West of the Nile River, Egypt. *Geocarto Int.* **2017**, *32*, 541–555. [[CrossRef](#)]
89. Reddy, G.P.O.; Mouli, K.C.; Srivastav, S.K.; Srinivas, C.V.; Maji, A.K. Evaluation of Ground Water Potential Zones Using Remote Sensing Data-A Case Study of Gaimukh Watershed, Bhandara District, Maharashtra. *J. Indian Soc. Remote Sens.* **2000**, *28*, 19–32. [[CrossRef](#)]
90. Senthilkumar, M.; Gnanasundar, D.; Arumugam, R. Identifying Groundwater Recharge Zones Using Remote Sensing & GIS Techniques in Amaravathi Aquifer System, Tamil Nadu, South India. *Sustain. Environ. Res.* **2019**, *29*, 15. [[CrossRef](#)]
91. Algaydi, B.A.M.; Subyani, A.M.; Hamza, M.H.M.M. Investigation of Groundwater Potential Zones in Hard Rock Terrain, Wadi Na'man, Saudi Arabia. *Groundwater* **2019**, *57*, 940–950. [[CrossRef](#)]
92. Adeyeye, O.A.; Ikpokonte, E.A.; Arabi, S.A. GIS-Based Groundwater Potential Mapping within Dengi Area, North Central Nigeria. *Egypt. J. Remote Sens. Sp. Sci.* **2019**, *22*, 175–181. [[CrossRef](#)]
93. Andualem, T.G.; Demeke, G.G. Groundwater Potential Assessment Using GIS and Remote Sensing: A Case Study of Guna Tana Landscape, Upper Blue Nile Basin, Ethiopia. *J. Hydrol. Reg. Stud.* **2019**, *24*, 100610. [[CrossRef](#)]
94. Ahmed, J.B., II; Mansor, S. Overview of the Application of Geospatial Technology to Groundwater Potential Mapping in Nigeria. *Arab. J. Geosci.* **2018**, *11*, 504. [[CrossRef](#)]
95. Yang, J.; Zhang, H.; Ren, C.; Nan, Z.; Wei, X.; Li, C. A Cross-Reconstruction Method for Step-Changed Runoff Series to Implement Frequency Analysis under Changing Environment. *Int. J. Environ. Res. Public Health* **2019**, *16*, 4345. [[CrossRef](#)] [[PubMed](#)]
96. Bhanja, S.N.; Mukherjee, A.; Rangarajan, R.; Scanlon, B.R.; Malakar, P.; Verma, S. Long-Term Groundwater Recharge Rates across India by in Situ Measurements. *Hydrol. Earth Syst. Sci.* **2019**, *23*, 711–722. [[CrossRef](#)]
97. Alogayell, H.M.; EL-Bana, E.M.M.; Abdelfattah, M. Groundwater Quality and Suitability Assessment for Irrigation Using Hydrogeochemical Characteristics and Pollution Indices: A Case Study of North Al-Quwayiyah Governorate, Central Saudi Arabia. *Water* **2023**, *15*, 3321. [[CrossRef](#)]

Disclaimer/Publisher's Note: The statements, opinions and data contained in all publications are solely those of the individual author(s) and contributor(s) and not of MDPI and/or the editor(s). MDPI and/or the editor(s) disclaim responsibility for any injury to people or property resulting from any ideas, methods, instructions or products referred to in the content.